Journal of Molecular Spectroscopy 405 (2024) 111947

Contents lists available at ScienceDirect

Journal of Molecular Spectroscopy

journal homepage: www.elsevier.com/locate/yjmsp

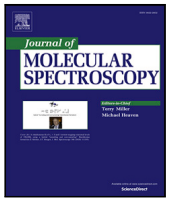

Article

MARVEL analysis of high-resolution rovibrational spectra of the $^{18}O^{12}C^{18}O$, $^{17}O^{12}C^{18}O$, and $^{18}O^{13}C^{18}O$ isotopologues of carbon dioxide

Ala'a A.A. Azzam [a], Sumaya A.A. Azzam [b], Karam A.A. Aburumman [a,b], Jonathan Tennyson [c,*], Sergei N. Yurchenko [c], Attila G. Császár [d,e], Tibor Furtenbacher [f]

[a] Department of Physics, The University of Jordan, Queen Rania St, Amman, Jordan
[b] Research Department, AstroJo Institute, Wasfi Al-Tal St, Amman, Jordan
[c] Department of Physics and Astronomy, University College London, Gower Street, London WC1E 6BT, UK
[d] ELTE Eötvös Loránd University, Institute of Chemistry, H-1117 Budapest, Pázmány Péter sétány 1/A, HUN-REN–ELTE Complex Chemical Systems Research Group, H-1532 Budapest, P.O. Box 32, Hungary
[e] Jet Propulsion Laboratory, California Institute of Technology, 4800 Oak Grove Drive, Pasadena, CA 91109, USA
[f] HUN-REN–ELTE Complex Chemical Systems Research Group, H-1532 Budapest, P.O. Box 32, Hungary

ARTICLE INFO

Keywords:
Empirical rovibrational energy levels
CO_2 isotopologues
Line positions
MARVEL

ABSTRACT

For three rare isotopologues of carbon dioxide, $^{18}O^{12}C^{18}O$ (828, according to a well-established shorthand notation), $^{17}O^{12}C^{18}O$ (728), and $^{18}O^{13}C^{18}O$ (838), 3923, 4318, and 1058 empirical rovibrational energy levels, respectively, are determined, using the MARVEL (Measured Active Rotational–Vibrational Energy Levels) protocol and code. For the isotopologues 828/728/838, the analysis of their spectroscopic network is based on 11 353(7665)/11 313(7700)/2155(1595) measured(unique) transitions, belonging to 165/113/50 vibrational bands, respectively. The measured transitions collected from the literature span the regions 953–12 570 cm^{-1} (for 828), 628–8197 cm^{-1} (for 728), and 600–7918 cm^{-1} (for 838). The number of critically evaluated and recommended energy levels of this study are 3923, 4318, and 1058 for the 828, 728, and 838 isotopologues of CO_2, respectively. Comparison of the empirical rovibrational energy levels determined in this study with their counterparts in two published databases, CDSD-2019, Ames-2021 and HITRAN shows very good overall agreement.

1. Introduction

Carbon dioxide, CO_2, is one of the most important constituents of a large number of planetary atmospheres. It has important role in the radiative balance of even the Earth's atmosphere, where it has a relatively low abundance compared to the atmospheres of the neighboring planets Venus and Mars. The rapidly increasing concentration of CO_2 in the Earth's atmosphere is of considerable concern for humanity and, consequently, the international scientific community [1].

Accurate knowledge of the spectroscopic properties of the carbon dioxide molecule, whether it is in itself or part of atmospheres of different constitution, is a minimum requirement for understanding the greenhouse effect and the evolution of planetary atmospheres. It is therefore important to have complete and accurate data sets helping CO_2-monitoring experiments, such as NASA's Orbiting Carbon Observatories OCO-2 and OCO-3 [2]. Given that the key, long-wavelength bands of the parent isotopologue, $^{12}C^{16}O_2$ (usually abbreviated as 626, following the well-accepted HITRAN [3] parlance, also employed in this paper), are largely saturated in the Earth's atmosphere [4], absorption by minor CO_2 isotopologues becomes a significant issue. This is made more important as any increase in the abundances of the minor isotopologues contributes more to radiative forcing than increases in the concentration of the parent isotopologue. Furthermore, as absorption by the minor species is optically thin, they are ideal candidates to monitor CO_2 column densities.

Research on CO_2 spectroscopy is very important to support atmospheric remote sensing of the terrestrial planets, such as Mars and Venus, where this gas is the principal constituent of the atmosphere (95% of the much thinner air in the case of Mars). The first spectroscopic observations of the atmosphere of Venus, with a resolution of 0.1 cm^{-1} [5], were performed in 1966. Several years later a higher resolution (0.015 cm^{-1}) spectrum of the atmosphere of Venus was obtained and analyzed [6,7]. The windows of the Venus atmosphere at 1.74 μm (5747 cm^{-1}) and 2.25 μm (4444 cm^{-1}) are of special importance, as a series of vibrational bands of CO_2 are located within these two regions. Strong selection rules apply for symmetric CO_2 species,

* Corresponding author.
E-mail addresses: alaa.azzam@ju.edu.jo (A.A. Azzam), j.tennyson@ucl.ac.uk (J. Tennyson).

https://doi.org/10.1016/j.jms.2024.111947
Received 12 June 2024; Received in revised form 30 August 2024; Accepted 5 September 2024
Available online 14 September 2024

whose relaxation in asymmetric isotopologues increases the importance of these trace species. Thus, the many more allowed rovibrational transitions of 728 make their relative contributions, in the two windows mentioned, significantly more important than they would be based on the relative abundance of this minor isotopologue.

In this study, we continue the investigation of the empirical rovibrational energy levels of carbon dioxide isotopologues, based on all the experimental transitions available in the literature. Recently, the empirical energy levels of $^{16}O^{12}C^{18}O$ (628) [8] and $^{16}O^{13}C^{16}O$ (636) [9] were determined by us using a procedure similar to what is followed in this study. The present contribution extends our work to two symmetric carbon dioxide isotopologues, $^{18}O^{12}C^{18}O$ (828) and $^{18}O^{13}C^{18}O$ (838), as well as to the asymmetric isotopologue $^{17}O^{12}C^{18}O$ (728). All these isotopologues have very low natural abundances, which are 0.000 395 7 % for 828 (the 7th most abundant CO_2 isotopologue), 0.000 147 2 % for 728 (the 8th in order), and 0.000 000 044 % for 838 (the 10th in order of CO_2 isotopologues). We also note that a MARVEL study of the parent isotopologue $^{16}O^{12}C^{16}O$ (626) has just been completed by our groups [10].

This paper is devoted to the construction of the most extensive empirical energy levels data set, calculated from line positions in high-resolution rovibrational absorption spectra, for the 828, 838, and 728 isotopologues of carbon dioxide (this study is part of an ongoing project of the three groups involved to determine the empirical energy levels for isotopologues of CO_2 involving ^{12}C, ^{13}C, ^{16}O, ^{17}O, and ^{18}O isotopes). Like the other subprojects, the empirical energy levels for the 828, 838, and 728 isotopologues are calculated using the MARVEL 4.0 (Measured Active Rotational–Vibrational Energy Levels) procedure [11–13], built upon the theory of spectroscopic networks [14, 15].

2. Notation and quantum numbers

CO_2 has three fundamental vibrational modes, conventionally denoted as ν_1, ν_2, and ν_3, associated with the vibrational quantum numbers $v_i, i = 1, 2$, and 3, respectively. The two-dimensional (degenerate) bending mode, ν_2, is characterized by an angular momentum, described by the quantum number ℓ_2. Herzberg's notation is often used to assign energy levels in triatomics; in this notation, the vibrational states of CO_2 are designated as (v_1, v_2^{ℓ}, v_3). For the CO_2 molecule with a linear equilibrium structure in its ground electronic state, there is a strong Fermi-resonance interaction between states $(v_1, (v_2 + 2)^{\ell}, v_3)$ and $(v_1 + 1, v_2^{\ell}, v_3)$. Therefore, it became customary to employ the so-called AFGL (Air Force Geophysics Laboratory) notation to denote the vibrational states and bands of CO_2 isotopologues. In the AFGL notation [16–18], the vibrational energy levels are designated by the quintuplet $(v_1, v_2, \ell_2, v_3, r)$, where r is the ranking index for states in Fermi resonance (the r index is used to distinguish the levels belonging to the same Fermi polyad). The lowest value of r, 1, is assigned to the energy level with the highest wavenumber (or frequency), and r increases for lower-energy levels. For example, the three vibrational states (20^00), (12^00), and (04^00) are in Fermi resonance with each other and have the AFGL vibrational descriptors (2 0 0 0 3), (2 0 0 0 2), and (2 0 0 0 1), respectively.

It is customary to use polyad numbers, P, to denote strongly interacting groups of vibrational states, decoupling them from the other vibrations, a useful concept especially when effective Hamiltonians are formed. P is not a quantum number, but it behaves like one. For carbon dioxide, based on the approximate relations of the harmonic frequencies, $\omega_1 \approx 2\omega_2$ and $\omega_3 \approx 3\omega_2$, the widely accepted definition of P, also utilized in this study, is $P = 2v_1 + v_2 + 3v_3$.

As usual in molecular spectroscopy, J is used to denote the quantum number associated with the rotational angular momentum of the CO_2 molecule. Transitions with $\Delta J = -1$ are called the P-branch transitions and those with $\Delta J = +1$ are called R-branch transitions, while the Q-branch transitions are associated with $\Delta J = 0$. P and R transitions occur in both parallel and perpendicular bands, while Q branch transitions only occur in parallel bands, where the direction refers to the change in the dipole moment driving the transition relative to the linear (equilibrium) molecule. For the symmetric isotopologues 828 and 838, half of the rotational levels are missing due to the Pauli exclusion principle: symmetric vibrational states (those with even v_3 values) only have even J levels, while anti-symmetric vibrational states (with odd v_3 values) have only odd J levels. Similarly, for states with even $J + \ell_2 + v_3$ the rotationless parity is 'e', while for states with odd $J + \ell_2 + v_3$ values the rotationless parity is 'f'. For the asymmetric 728 isotopologue, all J levels are present, and bands with $l_2 > 0$ display l-type doubling, giving both e and f levels for each J. Note that l-type doubling depends on J; for some J values, e and f lines sometimes become very close together and cannot be resolved. For all isotopologues levels with J smaller than l_2 cannot occur.

The upper and lower states involved in a transition are denoted as $'$ and $''$, respectively, and the P, R, and Q transitions are usually specified using the lower-state rotational quantum number (J''). For the purposes of the MARVEL analysis, each state is uniquely characterized using the set of descriptors $(v_1, v_2, \ell_2, v_3, r, J, e/f)$.

3. Marvel

The MARVEL procedure [11–13], used extensively during this study, starts with the careful collection, detailed examination, and subsequent validation of the positions of transitions in high-resolution (laboratory) spectra. The transitions collected are then used to construct a spectroscopic network (SN), whereby each energy level serves as a node, and the nodes are interconnected by the observed transitions. The SN built allows the determination of empirical energy-level values along with educated estimates for their uncertainties [19]. Unlike effective Hamiltonians, the MARVEL approach is model free. This has a number of advantages, in particular for the CO_2 molecule with its many resonances, MARVEL does not require any special measures or extra parameters to characterize levels perturbed by "accidental" interactions with those from nearby vibrational states.

Ideally, the experimentally observed transitions allow the creation of a well-connected SN, linking all transitions to the ground state (defined as the state with no rovibrational excitation), also called the root of the SN. However, due to the limited coverage offered by experimental data, usually this is not the case. Therefore, in practice, the SN becomes fragmented, resulting in a principal component, where all the nodes are linked to the root, and a number of isolated, so-called floating components with their own roots. The very nature of these floating components makes it uncertain whether their constituent lines align with all the other spectroscopic data, meaning that these lines are not validated at the end of a MARVEL analysis. When floating components contain a substantial number of transitions, it may be advantageous to connect them to the principal component(s) through accurately-known semi-empirical lines. In addition, in certain cases it is worth adding very precisely calculated lines to MARVEL datasets, lines which have uncertainties orders of magnitude smaller than the uncertainties of the measured transitions; thus, these calculated transitions can help to verify measured transitions.

The MARVEL protocol facilitates the detection of inconsistencies, that is lines which are in conflict with the correct data. This feature proves invaluable for identifying issues with experimental data usually coming from several sources, whether stemming from user mistakes during data collection and analysis, incorrect assignments, or the use of different naming conventions.

4. Results and discussion

The results obtained in this study for the three isotopologues of CO_2 studied will be discussed separately. Nevertheless, to save space, Table 1, describing the experimental sources of rovibrational transitions utilized during this study, as well as some of the figures, contain results for all three isotopologues.

Table 1
Experimental sources of rovibrational transitions of the isotopologues $^{18}O^{12}C^{18}O$, $^{17}O^{12}C^{18}O$ and $^{18}O^{13}C^{18}O$, and some characteristics of the lines they contain.[a].

Isotopologue	Source	Range/cm^{-1}	$A/V/D$	CSU	MSU
828	94MaChEvZi_Calc [20]	902.13–1120.62	142/142/0	1.8×10^{-6}	1.8×10^{-6}
	86BrSoFr_Calc [21]	913.45–1116.05	122/122/0	6.7×10^{-7}	6.7×10^{-7}
	99ClTeHuVa [22]	953.44–1101.70	20/20/0	2.5×10^{-4}	2.5×10^{-4}
	12LyKaJaLu [23]	1839.89–6882.94	798/798/0	1.0×10^{-3}	1.2×10^{-3}
	83EsRo [24]	2177.70–2356.28	541/541/0	4.0×10^{-4}	6.1×10^{-4}
	86EsSaRoVa [25]	2177.70–3678.03	677/677/0	1.0×10^{-3}	1.2×10^{-3}
	07ToMiBrDe [26]	2229.23–6883.13	1349/1349/0	2.1×10^{-3}	2.1×10^{-3}
	15ElSuMi_Calc [27]	2252.47–2346.65	67/67/0	2.4×10^{-6}	4.8×10^{-6}
	14BoJaLyTa [28]	3234.60–4680.88	460/460/0	3.0×10^{-4}	4.6×10^{-4}
	86EsRo [29]	3470.94–3678.03	136/136/0	4.0×10^{-4}	1.1×10^{-3}
	12JaGuLyKa [30]	3473.13–5009.21	106/106/0	5.6×10^{-4}	5.6×10^{-4}
	16VaKoMoKa [31]	4297.21–4378.09	75/75/0	1.0×10^{-3}	1.1×10^{-3}
	08WaPeTaSo [32]	4613.11–8162.85	1898/1898/0	1.0×10^{-3}	1.2×10^{-3}
	15BoJaLyTa [33]	4681.57–5018.43	231/231/0	1.7×10^{-4}	2.8×10^{-4}
	18KaCeMoKa [34]	5702.94–5878.26	667/667/0	1.0×10^{-3}	1.0×10^{-3}
	14KaCaMoKab [35]	5851.52–6883.26	2837/2837/0	1.0×10^{-3}	1.0×10^{-3}
	17KaCaKaTa [36]	6978.01–7917.58	1381/1381/0	1.0×10^{-3}	1.0×10^{-3}
	16SeSiLuBo [37]	11262.61–11335.04	47/47/0	8.0×10^{-3}	8.0×10^{-3}
	13PaLiLuLi [38]	12392.20–12569.33	83/83/0	3.0×10^{-3}	3.0×10^{-3}
728	80ReFlGo [39]	628.43–692.65	78/78/0	3.0×10^{-3}	4.7×10^{-3}
	99ClTeHuVa [22]	939.72–1105.03	86/86/0	5.0×10^{-5}	6.1×10^{-5}
	12LyKaJaLu [23]	1844.81–6908.44	3213/3213/0	1.0×10^{-3}	1.1×10^{-3}
	07ToMiBrDe [26]	2257.96–5040.78	696/696/0	1.1×10^{-3}	1.2×10^{-3}
	12JaGuLyKa [30]	2268.72–5043.60	393/393/0	5.6×10^{-4}	5.6×10^{-4}
	14ElSuMi [40]	2268.72–2355.62	55/55/0	3.0×10^{-6}	3.0×10^{-6}
	14BoJaLyTa [28]	3214.92–4681.26	1905/1905/0	3.0×10^{-4}	4.7×10^{-4}
	16VaKoMoKa [31]	4298.10–4342.86	44/44/0	2.0×10^{-3}	2.0×10^{-3}
	15BoJaLyTa [33]	4681.26–5270.38	983/983/0	2.1×10^{-4}	3.4×10^{-4}
	18KaCeMoKa [34]	5704.72–5878.70	397/397/0	1.0×10^{-3}	1.1×10^{-3}
	19MoKaPeTa [41]	5706.98–5849.97	563/563/0	1.0×10^{-3}	1.1×10^{-3}
	14KaCaMoKa [42]	5868.12–6908.44	1786/1786/0	1.0×10^{-3}	1.0×10^{-3}
	15JaBoLyTa [43]	6027.07–6235.26	171/171/0	5.6×10^{-4}	6.0×10^{-4}
	11VaKaHe [44]	6078.56–6100.14	40/40/0	2.0×10^{-3}	5.9×10^{-3}
	17KaCaKaTa [36]	6996.61–7808.67	761/761/0	1.0×10^{-3}	1.0×10^{-3}
	13GoHeLy [45]	8035.75–8196.67	142/142/0	2.0×10^{-3}	2.2×10^{-3}
838	80ReFlGo [39]	600.48–2282.35	118/118/0	4.0×10^{-3}	1.2×10^{-2}
	94MaChEvZi_Calc [20]	866.19–1062.79	142/142/0	2.6×10^{-6}	2.6×10^{-6}
	86BrSoFr_Calc [21]	876.88–1058.51	122/122/0	5.7×10^{-7}	5.7×10^{-7}
	08ToMiBrDe [46]	2180.89–4888.38	321/321/0	1.1×10^{-3}	1.2×10^{-3}
	12LyKaJaLu [23]	2181.95–3473.40	249/249/0	1.0×10^{-3}	1.1×10^{-3}
	14BoJaLyTa [28]	3384.72–3572.99	141/141/0	3.0×10^{-4}	3.2×10^{-4}
	16VaKoMoKa [31]	4318.83–4377.24	25/25/0	1.0×10^{-3}	2.0×10^{-3}
	15BoJaLyTa [33]	4746.17–4755.53	7/7/0	6.1×10^{-4}	6.1×10^{-4}
	18KaCeMoKa [34]	5703.23–5877.05	184/184/0	1.0×10^{-3}	1.0×10^{-3}
	14KaCaMoKab [35]	5867.95–6688.20	538/538/0	1.0×10^{-3}	1.1×10^{-3}
	08PePeCa [47]	5880.44–6688.20	170/170/0	1.3×10^{-3}	1.5×10^{-3}
	17KaCaKaTa [36]	7057.01–7917.09	350/350/0	1.0×10^{-3}	1.0×10^{-3}
	10CaSoMoPe [48]	7785.13–7916.86	52/52/0	8.0×10^{-4}	1.0×10^{-3}

[a] $A/V/D$ = Available/Validated/Deleted transitions. CSU = Average claimed source uncertainty. MSU = Average MARVEL-suggested source uncertainty.

4.1. $^{18}O^{12}C^{18}O$ (828)

As mentioned in Section 3, it is sometimes useful and practical to add accurate calculated transitions to experimental data collected for a MARVEL analysis. For 828, out of the 11 654 transitions in our database (see Supplementary Information), there are 11 306 experimentally measured transitions [22–26,28–38], spanning the region 953–12 570 cm^{-1}, 331 highly accurate calculated transitions from three sources [20,21,27], and 17 Carbon Dioxide Spectroscopic Databank (CDSD-19) [49] transitions.

A considerable number of experimental spectra have been published for the 828 isotopologue of carbon dioxide between 1983 and 2018 [22–26,28–38]. Some of the most important characteristics of the literature sources utilized during this study are summarized in Table 1. The total number of the known experimental transitions is 7665 with the maximum polyad number P_{max} = 17. These transitions determine 3923 empirical rovibrational energy levels which are represented by black dots in Fig. 1. These empirical energy levels have J_{max} = 87, see Figs. 2 and 3. To minimize the number of measured transitions which are rejected during the MARVEL analysis, we had to relabel seven transitions of the source 08WaPeTaSo [32]. The wavenumbers of the transitions in question could be found, with almost perfect matches, in the database CDSD-19 [49]; thus, we used the labels of these transitions in our MARVEL input file (the tag of these lines contains 'relab').

The SN of the experimentally measured transitions of 828 contains six larger floating components, with 145, 16, 15, 11, 10, and 10 rovibrational quantum states. To connect these FCs to the principal component, we used calculated energy levels from CDSD-19 [49]. Using these energy values of CDSD-19, we added 17 artificial transitions, with 5×10^{-3} cm^{-1} uncertainty, to our experimental database. These transitions are tagged '19CDSD' in the transitions file (see Supplementary Material).

4.2. $^{17}O^{12}C^{18}O$ (728)

For 728, rovibrational transitions, spanning the region 628–8197 cm^{-1}, have been recorded and analyzed by a number of research groups [22,23,26,28,30,31,33,34,36,39–45]. We were able

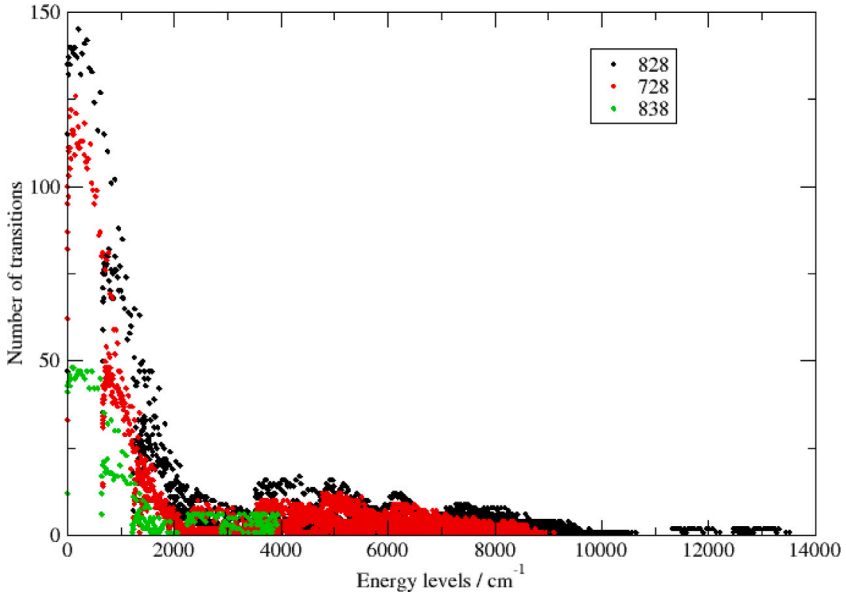

Fig. 1. Number of transitions used during the MARVEL analysis to determine each energy level versus the energy levels calculated for the carbon dioxide isotopologues $^{18}O^{12}C^{18}O$ (828), $^{17}O^{12}C^{18}O$ (728), and $^{18}O^{13}C^{18}O$ (838).

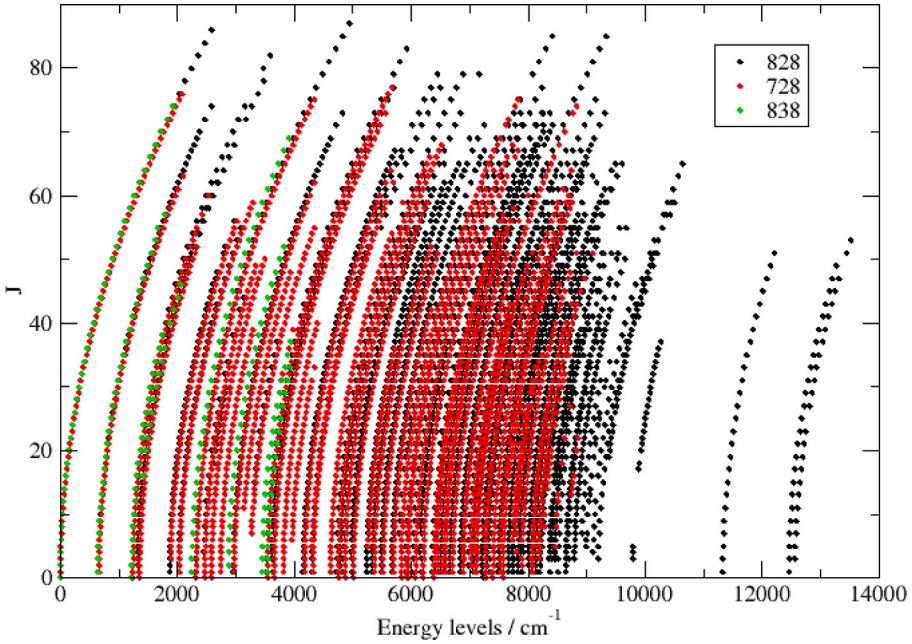

Fig. 2. Rotational quantum number, J, for each calculated energy level versus the energy levels calculated using MARVEL for the $^{18}O^{12}C^{18}O$ (828), $^{17}O^{12}C^{18}O$ (728), and $^{18}O^{13}C^{18}O$ (838) isotopologues of carbon dioxide.

to collect 11 353 transitions for this isotopologue, of which 7700 are unique. For the observed transitions, $P_{max} = 11$. The middle part of Table 1 summarizes characteristics of the 16 literature sources utilized. In this study, 4318 empirical rovibrational energy levels could be determined for 728 using all the collected observed transitions, see the red dots of Fig. 1. These empirical energy levels have $J_{max} = 78$, see Fig. 2, and $P_{max} = 13$, see Fig. 3.

The SN of the experimentally measured transitions of 728 contains five large FCs, among them two are unusually large. These floating components contain 250, 230, 15, 10, and 10 rovibrational energy levels. To connect these floating components to the principal component, we used, once again, the calculated energy levels of CDSD-19 [49]. Using the energy values of CDSD-19, we created 26 artificial transitions, with 5×10^{-3} cm^{-1} uncertainty, tagged '19CDSD' in the transitions file (see Supplementary Information).

4.3. $^{18}O^{13}C^{18}O$ (838)

In the case of the 838 isotopologue of carbon dioxide, we could collect 2155 experimentally measured transitions from the literature [23,28,31,33–36,39,46–48], while the number of unique transitions is only 1595 (for details, see the lower part of Table 1). Beyond the experimental results, we added 264 calculated lines from two sources [20,21] to the MARVEL 838 database, since the accuracy of these calculated lines

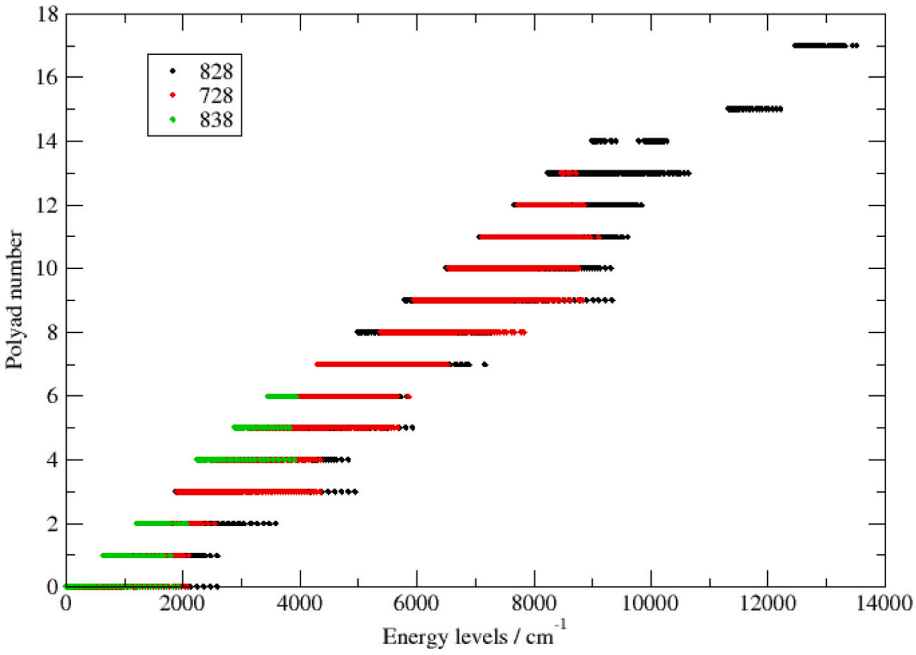

Fig. 3. Polyad number ($P = 2v_1 + v_2 + 3v_3$) for each calculated energy level for $^{18}O^{12}C^{18}O$ (828), $^{17}O^{12}C^{18}O$ (728), and $^{18}O^{13}C^{18}O$ (838) versus the energy levels calculated using MARVEL.

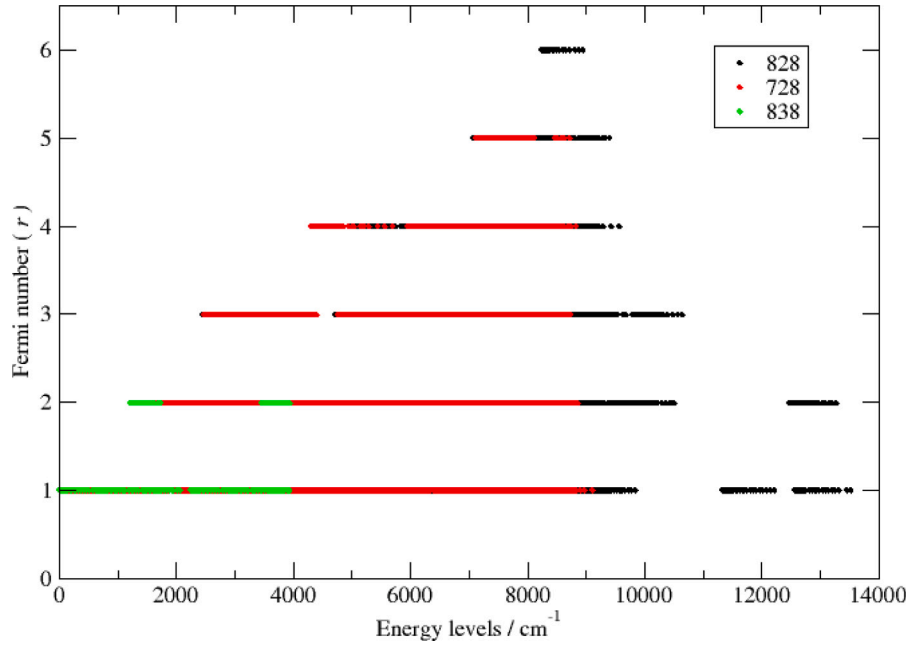

Fig. 4. Fermi number, r, for each calculated energy level versus the energy levels calculated using MARVEL for the carbon dioxide isotopologues $^{18}O^{12}C^{18}O$ (828), $^{17}O^{12}C^{18}O$ (728), and $^{18}O^{13}C^{18}O$ (838).

is much better than that of some of the measured lines. The transitions detected span the wavenumber range 601–7918 cm^{-1}, with P_{max} = 11. The observed transitions determine 1058 empirical rovibrational energy levels, see the green dots of Fig. 1. These empirical energy levels are characterized by $J_{max} = 75$, see Fig. 2, and $P_{max} = 16$, see Fig. 3.

The SN of the experimentally measured transitions of 838 contains two large floating components. These components contain 198 and 11 rovibrational energy levels. To connect these floating components to the principal component, we used, similar to the two previous cases, calculated energy levels from CDSD-19 [49]. Using the energy values of CDSD-19, we created seven artificial transitions (with 5×10^{-3} cm^{-1} uncertainty); they are tagged as '19CDSD' in the transitions file.

Fig. 4 illustrates the distribution of the derived energy levels of the three CO_2 isotopologues over Fermi resonances as characterized by the resonance number r.

5. Comparison with databases CDSD-19, Ames-2021, and HITRAN 2020

Comparing empirical energy levels with energy levels available in different spectroscopic databases is always insightful and can serve

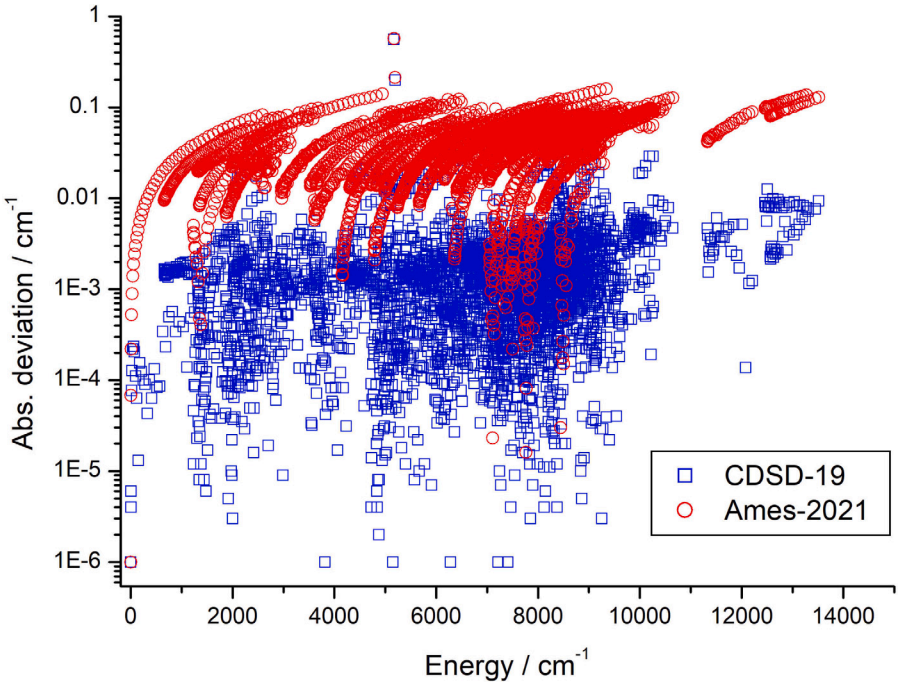

Fig. 5. Comparison between rovibrational energies of the present $^{18}O^{12}C^{18}O$ dataset and those of CDSD-2019 [49] (blue squares) and Ames-2021 [50] (red circles).

multiple purposes. For the carbon dioxide isotopologues studied, this comparison can be done with respect to the databases CDSD-19 [49], Ames-2021 [50], and HITRAN 2020 [3].

5.1. $^{18}O^{12}C^{18}O$ (828)

Fig. 5 shows the absolute deviations between MARVEL and the CDSD-2019 and Ames-2021 datasets. Note that for Ames-2021 we compare with their results from variational nuclear motion calculations; in practice the final Ames CO_2 line lists use CDSD data to improve their line positions. Clearly, the agreement should be considered to be (a) good between our dataset and CDSD-2019, with an average deviation as small as 2×10^{-3} cm^{-1}, and (b) reasonable with Ames-2021, with an average deviation as large as 4×10^{-2} cm^{-1}. As Fig. 5 shows, there are two energy levels with deviations from the CDSD-19 results larger than 0.1 cm^{-1}. These two energy levels were determined from a single measured transition of the source 07ToMiBrDe [26], and the experimental uncertainty of these measured lines is larger than 0.1 cm^{-1}. The line-by-line comparison with data in the CDSD-19 database shows that the largest differences are with the measured transitions of the sources 16VaKoMoKa [31] and 17KaCaKaTa [36].

A line-by-line comparison was also made with the HITRAN 2020 [3] database. The 828 database of HITRAN 2020 contains 10 497 transitions in the 482.8–8162.7 cm^{-1} region. We find 4902 experimentally measured line not present in HITRAN 2020 but validated in the present study; in general these lines are not strong enough to meet the HITRAN 296 K, natural-abundance intensity cut-off; these lines were published in the following four sources: 08WaPeTaSo [32], 14KaCaMoKab [35], 17KaCaKaTa [36], and 18KaCeMoKa [34].

5.2. $^{17}O^{12}C^{18}O$ (728)

Fig. 6 shows the absolute deviations between the empirical (MARVEL) energy levels of the isotopologue 728 and their counterparts in the CDSD-19 and AMES-2021 databases. As seen in Fig. 6, the agreement is significantly better with CDSD-2019, with an average deviation of 1×10^{-3} cm^{-1}, than with Ames-2021, where the average deviation is 2.4×10^{-2} cm^{-1}. This is an unsurprising result for both 828 and 728 as the CDSD-19 energies are semi-empirical in nature.

For 728, the HITRAN 2020 dataset lists 14 623 transitions in the region 498.6–8193.2 cm^{-1}. The HITRAN 2020 database contains more lines than our experimental database, which actually has 7700 unique transitions, a line-by-line comparison shows that 3468 experimentally measured transitions are not included in the HITRAN 2020 database, generally because they are too weak to be considered important. Most of these missing line are published in the sources 12LyKaJaLu [23], 14BoJaLyTa [28], 14KaCaMoKa [42], 17KaCaKaTa [36], and 18KaCeMoKa [34].

5.3. $^{18}O^{13}C^{18}O$ (838)

Fig. 7 shows the absolute deviations between the empirical (MARVEL) energies and the corresponding entities in the CDSD-19 and AMES-2021 databases. As seen for the 828 and 728 isotopologues, the empirical rovibrational energy levels of this study show better agreement with the CSDS-19 data, with an average deviation of 1.4×10^{-3} cm^{-1} cm^{-1}, than with the Ames-2021 data, with an average deviation of 4.5×10^{-2} cm^{-1} cm^{-1}. Thus, we can conclude that we find basically the same average deviations between the empirical energy levels of this study and those of CDSD-19 and AMES-2021 for all three carbon dioxide isotopologues.

Comparing our experimental lines with the 838 lines present in the HITRAN 2020 database, containing 2926 transitions in the 539.6–6687.0 cm^{-1} region, we find 723 additional, weak lines. The experimental lines missing from HITRAN 2020 were published in the sources 08PePeCa [47], 14KaCaMoKab [35], and 18KaCeMoKa [34].

6. Summary and conclusions

This paper is devoted to a comprehensive, critical, line-by-line analysis of all available measured and assigned rovibrational transitions corresponding to the ground electronic state of three minor isotopologues of carbon dioxide, $^{18}O^{12}C^{18}O$ (828), $^{17}O^{12}C^{18}O$ (728), and $^{18}O^{13}C^{18}O$ (838). Our detailed and careful analysis utilized the

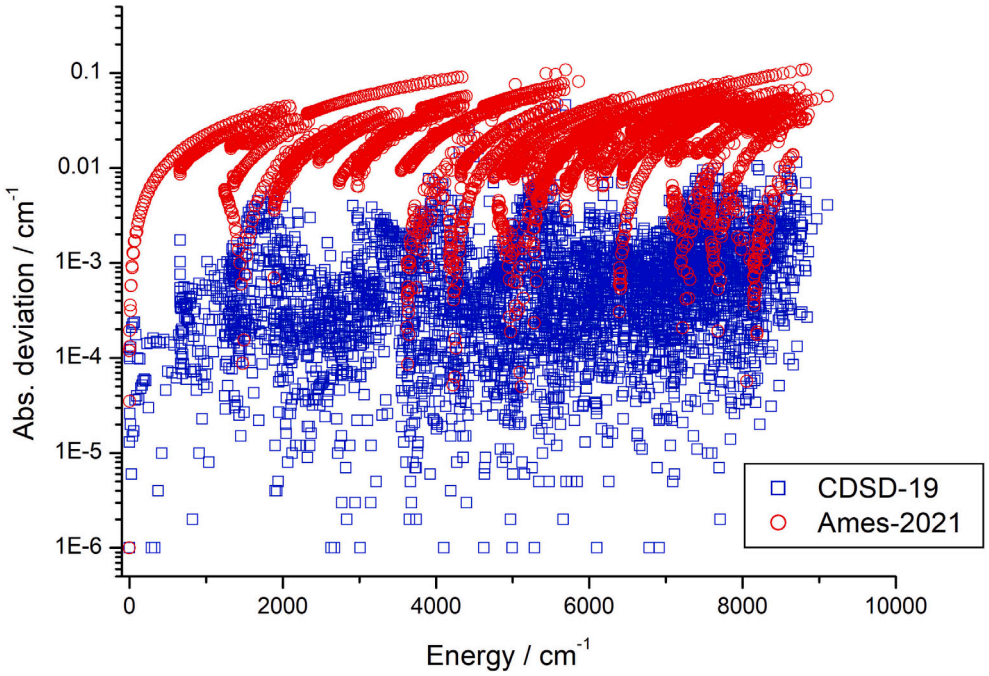

Fig. 6. Comparison between rovibrational energies of the present $^{17}O^{12}C^{18}O$ dataset and those of CDSD-2019 [49] (blue squares) and Ames-2021 [50] (red circles).

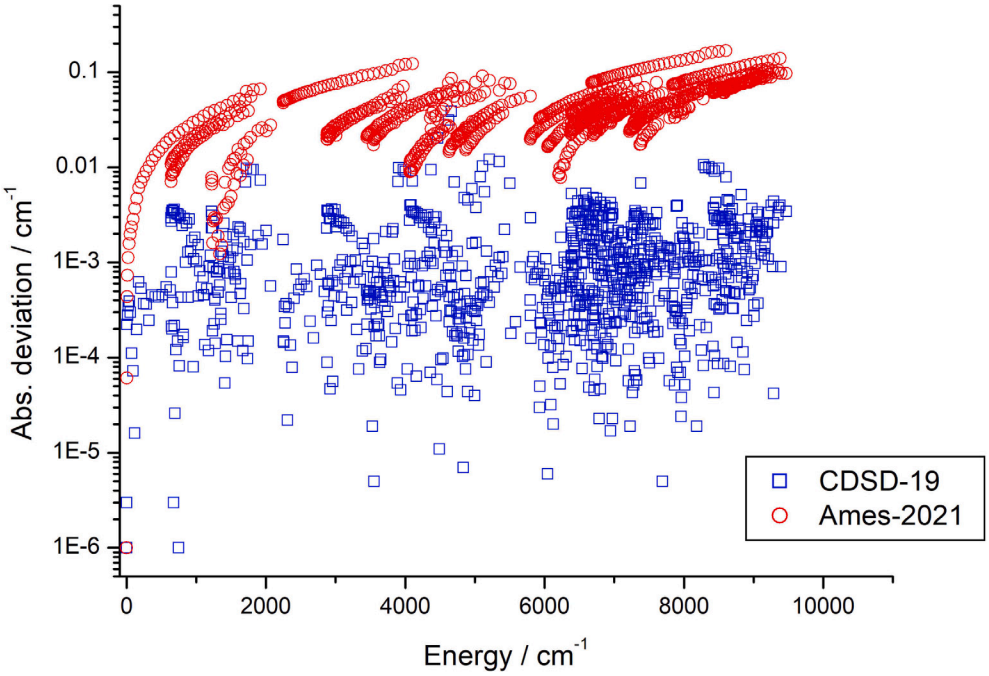

Fig. 7. Comparison between rovibrational energies of the present $^{18}O^{13}C^{18}O$ dataset and those of CDSD-2019 [49] (blue squares) and Ames-2021 [50] (red circles).

MARVEL algorithm [11–13] and the latest version of the associated code.

In total, 11 654 mostly experimentally measured transitions were collected from the literature for $^{18}O^{12}C^{18}O$. This dataset contains 7482 unique transitions, covers the wavenumber range of 953 – 12 570 cm^{-1}, and can be characterized by J_{max} = 87 and P_{max} = 17. This set of transitions yields 3923 empirical (MARVEL) energy levels. The average uncertainty of the empirical energy levels, derived from the experimental uncertainties of the transitions, is 2×10^{-3} cm^{-1}. Comparison of these energy levels with their counterparts in the CDSD-19 [49] and NASA Ames-2021 [50] databases reveals an average difference of 2×10^{-3} and 4×10^{-2} cm^{-1}, respectively.

For the eighth most abundant isotopologue of carbon dioxide, $^{17}O^{12}C^{18}O$, 11 339 mostly experimentally measured transitions were

collected, covering the wavenumber range of 628–8197 cm^{-1}, with $J_{max} = 78$ and $P_{max} = 13$. The dataset assembled contains 7700 transitions with unique assignments. The transition set of the 728 isotopologue yielded 4318 empirical (MARVEL) energy levels. The average uncertainty of the empirical energy levels is 1.6×10^{-3} cm^{-1}. Comparison of the empirical energy levels of this study with the CDSD-19 [49] and NASA Ames-2021 [50] results reveals average differences of 1×10^{-3} and 2.4×10^{-2} cm^{-1}, respectively.

In the case of the 838 isotopologue of carbon dioxide, 2426 mostly experimentally measured transitions were collected from the literature. The dataset assembled covers the wavenumber range of 601–7918 cm^{-1} with $J_{max} = 75$ and $P_{max} = 16$. These transitions correspond to 1595 unique assignments. The number of empirical energy levels determined is 1058. Comparison of these energy levels with the corresponding CDSD-19 [49] and the NASA Ames-2021 [50] data reveals average differences of 1.4×10^{-3} and 4.5×10^{-2} cm^{-1}, respectively.

Finally, we note, that accurate, computed *ab initio* intensities are available for both symmetric [51] and asymmetric [52] minor isotopologues of CO_2. This means that by combining these intensities with the empirical energies generated here, one can build highly accurate line lists.

CRediT authorship contribution statement

Ala'a A.A. Azzam: Writing – review & editing, Validation, Investigation, Formal analysis, Data curation, Conceptualization. **Sumaya A.A. Azzam:** Visualization, Formal analysis. **Karam A.A. Aburumman:** Investigation, Formal analysis. **Jonathan Tennyson:** Writing – original draft, Methodology, Funding acquisition, Data curation, Conceptualization. **Sergei N. Yurchenko:** Writing – review & editing, Validation, Investigation. **Attila G. Császár:** Writing – review & editing, Supervision, Formal analysis, Conceptualization. **Tibor Furtenbacher:** Software, Methodology, Formal analysis, Conceptualization.

Declaration of competing interest

The authors declare no conflict of interest

Data availability

All data is supplied as supplementary material to the article.

Acknowledgments

The authors thank STFC for funding the UK – Jordan collaboration under the Newton Fund (grant ST/T001429/1). JT acknowledges the support of the European Research Council (ERC) under the European Union's Horizon 2020 research and innovation programme through Advance Grant number 883830. AGC received support from NKFIH (grant no. K138233). The joint work between the Budapest and London groups received support from the COST Action COSY (Confined Molecular Systems, CA21101). AGC is grateful to the Fulbright Foundation for funding his stay at JPL [Jet Propulsion Laboratory, California Institute of Technology, under a contract with the National Aeronautics and Space Administration (NASA)] and to his host, Dr. Brian Drouin, for useful discussions. We also thank Dunia Alatoom and Mohammad Taha I. Ibrahim for help with the initial data collection.

Appendix A. Supplementary data

Supplementary material related to this article can be found online at https://doi.org/10.1016/j.jms.2024.111947.

References

[1] K. Calvin, D. Dasgupta, G. Krinner, A. Mukherji, P.W. Thorne, C. Trisos, J. Romero, P. Aldunce, K. Barrett, G. Blanco, W.W.L. Cheung, S. Connors, F. Denton, A. Diongue-Niang, D. Dodman, M. Garschagen, O. Geden, B. Hayward, C. Jones, F. Jotzo, T. Krug, R. Lasco, Y.-Y. Lee, V. Masson-Delmotte, M. Meinshausen, K. Mintenbeck, A. Mokssit, F.E.L. Otto, M. Pathak, A. Pirani, E. Poloczanska, H.-O. Pörtner, A. Revi, D.C. Roberts, J. Roy, A.C. Ruane, J. Skea, P.R. Shukla, R. Slade, A. Slangen, Y. Sokona, A.A. Sörensson, M. Tignor, D. van Vuuren, Y.-M. Wei, H. Winkler, P. Zhai, Z. Zommers, J.-C. Hourcade, F.X. Johnson, S. Pachauri, N.P. Simpson, C. Singh, A. Thomas, E. Totin, A. Alegría, K. Armour, B. Bednar-Friedl, K. Blok, G. Cissé, F. Dentener, S. Eriksen, E. Fischer, G. Garner, C. Guivarch, M. Haasnoot, G. Hansen, M. Hauser, E. Hawkins, T. Hermans, R. Kopp, N. Leprince-Ringuet, J. Lewis, D. Ley, C. Ludden, L. Niamir, Z. Nicholls, S. Some, S. Szopa, B. Trewin, K.-I. van der Wijst, G. Winter, M. Witting, A. Birt, M. Ha, IPCC, 2023: climate change 2023: synthesis report, in: core writing team, H. Lee, J. Romero (Eds.), Contribution of Working Groups I, II and III to the Sixth Assessment Report of the Intergovernmental Panel on Climate Change, Tech. rep., IPCC, Geneva, Switzerland, 2023.

[2] J.M. Hobbs, B.J. Drouin, F. Oyafuso, V.H. Payne, M.R. Gunson, J. McDuffie, E.J. Mlawer, Spectroscopic uncertainty impacts on OCO-2/3 retrievals of XCO_2, J. Quant. Spectrosc. Radiat. Transfer 257 (2020) 107360, http://dx.doi.org/10.1016/j.jqsrt.2020.107360.

[3] I.E. Gordon, L.S. Rothman, R.J. Hargreaves, R. Hashemi, E.V. Karlovets, F.M. Skinner, E.K. Conway, C. Hill, R.V. Kochanov, Y. Tan, P. Wcisło, A.A. Finenko, K. Nelson, P.F. Bernath, M. Birk, V. Boudon, A. Campargue, K.V. Chance, A. Coustenis, B.J. Drouin, J.M. Flaud, R.R. Gamache, J.T. Hodges, D. Jacquemart, E.J. Mlawer, A.V. Nikitin, V.I. Perevalov, M. Rotger, J. Tennyson, G.C. Toon, H. Tran, V.G. Tyuterev, E.M. Adkins, A. Baker, A. Barbe, E. Canè, A.G. Császár, A. Dudaryonok, O. Egorov, A.J. Fleisher, H. Fleurbaey, A. Foltynowicz, T. Furtenbacher, J.J. Harrison, J.M. Hartmann, V.M. Horneman, X. Huang, T. Karman, J. Karns, S. Kassi, I. Kleiner, V. Kofman, F. Kwabia-Tchana, N.N. Lavrentieva, T.J. Lee, D.A. Long, A.A. Lukashevskaya, O.M. Lyulin, V.Y. Makhnev, W. Matt, S.T. Massie, M. Melosso, S.N. Mikhailenko, D. Mondelain, H.S.P. Müller, O.V. Naumenko, A. Perrin, O.L. Polyansky, E. Raddaoui, P.L. Raston, Z.D. Reed, M. Rey, C. Richard, R. Tóbiás, I. Sadiek, D.W. Schwenke, E. Starikova, K. Sung, F. Tamassia, S.A. Tashkun, J. Vander Auwera, I.A. Vasilenko, A.A. Vigasin, G.L. Villanueva, B. Vispoel, G. Wagner, A. Yachmenev, S.N. Yurchenko, The HITRAN2020 molecular spectroscopic database, J. Quant. Spectrosc. Radiat. Transfer 277 (2022) 107949, http://dx.doi.org/10.1016/j.jqsrt.2021.107949.

[4] K.P. Shine, G.E. Perry, Radiative forcing due to carbon dioxide decomposed into its component vibrational bands, Q. J. R. Meteorol. 149 (2023) 1856–1866, http://dx.doi.org/10.1002/qj.4485.

[5] J.-P. Maillard, J.R. Connes, P. Connes, Atlas des spectres dans le proche infrarouge de Vénus, Mars, Jupiter et Saturne: Near infrared spectra of Venus, Mars, Jupiter and Saturn, Centre national de la recherche scientifique, 1969.

[6] P. Connes, G. Michel, High-resolution Fourier spectra of stars and planets, Astrophys. J. 190 (1974) L29–L32, http://dx.doi.org/10.1086/181496.

[7] J.-Y. Mandin, Interpretation of the CO_2 absorption bands observed in the Venus infrared spectrum between 1 and 2.5μm, J. Mol. Spectrosc. 67 (1977) 304–321, http://dx.doi.org/10.1016/0022-2852(77)90044-3.

[8] D. Alatoom, M.T.I. Ibrahim, T. Furtenbacher, A.G. Császár, M. Alghizzawi, S.N. Yurchenko, A.A.A. Azzam, J. Tennyson, MARVEL analysis of high-resolution rovibrational spectra of $^{16}O^{12}C^{18}O$, J. Comput. Chem. (2024) http://dx.doi.org/10.1002/jcc.27453.

[9] M.T.I. Ibrahim, D. Alatoom, T. Furtenbacher, A.G. Császár, S.N. Yurchenko, A.A.A. Azzam, J. Tennyson, MARVEL analysis of high-resolution rovibrational spectra of $^{16}O^{13}C^{16}O$, J. Comput. Chem. 45 (2024) 969–984, http://dx.doi.org/10.1002/jcc.27266.

[10] A.A.A. Azzam, B.M.J. Abou Doud, M.Q.A. Shersheer, B.K.M. Almasri, C.N.M. Bader, A.M.H.A. Baraa O. A. K.H. Musleh and, A.W.M. Al Shatarat, B.I.M. Qattan, L.H.M. Hamamsy, A.O.G. Saafneh, M.N.A. ALso'ub, M.M.A. Alkhashashneh, H.O.M. Al-Zawahra, A. Abu Khudair, M.Z.J. Abeido, D. Alatoom, M.T.I. Ibrahim, J. Tennyson, S.N. Yurchenko, A.G. Császár, T. Furtenbacher, MARVEL analysis of high-resolution rovibrational spectra of $^{16}O^{12}C^{16}O$, J. Quant. Spectrosc. Radiat. Transfer (2024).

[11] A.G. Császár, G. Czakó, T. Furtenbacher, E. Mátyus, An active database approach to complete rotational–vibrational spectra of small molecules, Annu. Rep. Comput. Chem. 3 (2007) 155–176, http://dx.doi.org/10.1016/S1574-1400(07)03009-5.

[12] T. Furtenbacher, A.G. Császár, J. Tennyson, MARVEL: measured active rotational–vibrational energy levels, J. Mol. Spectrosc. 245 (2007) 115–125, http://dx.doi.org/10.1016/j.jms.2007.07.005.

[13] T. Furtenbacher, A.G. Császár, MARVEL: measured active rotational-vibrational energy levels. II. Algorithmic improvements, J. Quant. Spectrosc. Radiat. Transf 113 (2012) 929–935, http://dx.doi.org/10.1016/j.jqsrt.2012.01.005.

[14] A.G. Császár, T. Furtenbacher, Spectroscopic networks, J. Mol. Spectrosc. 266 (2011) 99–103, http://dx.doi.org/10.1016/j.jms.2011.03.031.

[15] T. Furtenbacher, A.G. Császár, The role of intensities in determining characteristics of spectroscopic networks, J. Mol. Struct. 1009 (2012) 123–129, http://dx.doi.org/10.1016/j.molstruc.2011.10.057.

[16] G. Amat, M. Pimbert, On Fermi resonance in carbon dioxide, J. Mol. Spectrosc. 16 (1965) 278–290, http://dx.doi.org/10.1016/0022-2852(65)90123-2.

[17] L.S. Rothman, L.D.G. Young, Infrared energy levels and intensities of carbon dioxide-II, J. Quant. Spectrosc. Radiat. Transfer 25 (1981) 505–524, http://dx.doi.org/10.1016/0022-4073(81)90026.

[18] R.A. Toth, L.R. Brown, C.E. Miller, V. Malathy Devi, D.C. Benner, Spectroscopic database of CO_2 line parameters: 4300 – 7000 cm^{-1}, J. Quant. Spectrosc. Radiat. Transfer 109 (2008) 906–921, http://dx.doi.org/10.1016/j.jqsrt.2007.12.004.

[19] J. Tennyson, T. Furtenbacher, S.N. Yurchenko, A.G. Császár, Empirical rovibrational energy levels for nitrous oxide, J. Quant. Spectrosc. Radiat. Transfer 316 (2024) 108902, http://dx.doi.org/10.1016/j.jqsrt.2024.108902.

[20] A.G. Maki, C.C. Chou, K.M. Evenson, L.R. Zink, J.T. Shy, Improved molecular constants and frequencies for the CO_2 laser from new high-J regular and hot-band frequency measurements, J. Mol. Spectrosc. 167 (1994) 211–224, http://dx.doi.org/10.1006/jmsp.1994.1227.

[21] L. Bradley, K. Soohoo, C. Freed, Absolute frequencies of lasing transitions in nine CO_2 isotopic species, IEEE J. Quantum Electron. 22 (1986) 234–267, http://dx.doi.org/10.1109/JQE.1986.1072967.

[22] C. Claveau, J.-L. Teffo, D. Hurtmans, A. Valentin, R.R. Gamache, Line positions and absolute intensities in the laser bands of carbon-12 oxygen-17 isotopic species of carbon dioxide, J. Mol. Spectrosc. 193 (1999) 15–32, http://dx.doi.org/10.1006/jmsp.1998.7704.

[23] O.M. Lyulin, E.V. Karlovets, D. Jacquemart, Y. Lu, A.W. Liu, V.I. Perevalov, Infrared spectroscopy of^{17}O- and^{18}O-enriched carbon dioxide in the 1700 – 8300 cm^{-1} wavenumber region, J. Quant. Spectrosc. Radiat. Transfer 113 (2012) 2167–2181, http://dx.doi.org/10.1016/j.jqsrt.2012.06.028.

[24] M.P. Esplin, L.S. Rothman, Spectral measurements of high temperature isotopic carbon dioxide in the 4.3 μm region, J. Mol. Spectrosc. 100 (1983) 193–204, http://dx.doi.org/10.1016/0022-2852(83)90036-X.

[25] M.P. Esplin, H. Sakai, L.S. Rothman, G.A. Vanasse, W.M. Barowy, R.J. Huppi, Carbon Dioxide Line Positions in the 2.8 and 4.3μm Regions at 800 Kelvin, Tech. Rep. AFGL-TR-86-0046, Utah State University, 1986, https://apps.dtic.mil/sti/citations/ADA173808.

[26] R.A. Toth, C.E. Miller, L.R. Brown, V. Malathy Devi, D.C. Benner, Line positions and strengths of $^{16}O^{12}C^{18}O$, $^{18}O^{12}C^{18}O$ and $^{17}O^{12}C^{18}O$ between 2200 and 7000 cm^{-1}, J. Mol. Spectrosc. 243 (2007) 43–61, http://dx.doi.org/10.1016/j.jms.2007.03.005.

[27] B.M. Elliott, K. Sung, C.E. Miller, FT-IR spectra of ^{18}O-, and ^{13}C-enriched CO_2 in the ν_3 region: High accuracy frequency calibration and spectroscopic constants for $^{16}O^{12}C^{18}O$, $^{18}O^{12}C^{18}O$, and $^{16}O^{13}C^{16}O$, J. Mol. Spectrosc. 312 (2015) 78–86, http://dx.doi.org/10.1016/j.jms.2015.02.007.

[28] Y.G. Borkov, D. Jacquemart, O.M. Lyulin, S.A. Tashkun, V.I. Perevalov, Infrared spectroscopy of ^{17}O- and ^{18}O-enriched carbon dioxide: Line positions and intensities in the 3200 – 4700 cm^{-1} region. Global modeling of the line positions of $^{16}O^{12}C^{17}O$ and $^{17}O^{12}C^{17}O$, J. Quant. Spectrosc. Radiat. Transfer 137 (2014) 57–76, http://dx.doi.org/10.1016/j.jqsrt.2013.11.008.

[29] M.P. Esplin, L.S. Rothman, Spectral measurements of high-temperature isotopic carbon dioxide in the 4.5- and 2.8-μm regions, J. Mol. Spectrosc. 116 (1986) 351–363, http://dx.doi.org/10.1016/0022-2852(86)90132-3.

[30] D. Jacquemart, F. Gueye, O.M. Lyulin, E.V. Karlovets, D. Baron, V.I. Perevalov, Infrared spectroscopy of CO_2 isotopologues from 2200 to 7000 cm^{-1}: I—Characterizing experimental uncertainties of positions and intensities, J. Quant. Spectrosc. Radiat. Transfer 113 (2012) 961–975, http://dx.doi.org/10.1016/j.jqsrt.2012.02.020.

[31] S. Vasilchenko, M. Konefal, D. Mondelain, S. Kassi, P. Čermák, S.A. Tashkun, V.I. Perevalov, A. Campargue, The CO_2 absorption spectrum in the 2.3μm transparency window by high sensitivity CRDS: (I) Rovibrational lines, J. Quant. Spectrosc. Radiat. Transfer 184 (2016) 233–240, http://dx.doi.org/10.1016/j.jqsrt.2016.07.002.

[32] L. Wang, V.I. Perevalov, S.A. Tashkun, K.-F. Song, S.-M. Hu, Fourier transform spectroscopy of $^{12}C^{18}O_2$ and $^{16}O^{12}C^{18}O$ in the 3800–8500 cm^{-1} region and the global modeling of the absorption spectrum of$^{12}C^{18}O_2$, J. Mol. Spectrosc. 247 (2008) 64–75, http://dx.doi.org/10.1016/j.jms.2007.09.015.

[33] Y.G. Borkov, D. Jacquemart, O.M. Lyulin, S.A. Tashkun, V.I. Perevalov, Infrared spectroscopy of^{17}O- and^{18}O-enriched carbon dioxide: Line positions and intensities in the 4681 – 5337 cm^{-1} region, J. Quant. Spectrosc. Radiat. Transfer 159 (2015) 1–10, http://dx.doi.org/10.1016/j.jqsrt.2015.02.019.

[34] E.V. Karlovets, P. Čermák, D. Mondelain, S. Kassi, A. Campargue, S.A. Tashkun, V.I. Perevalov, Analysis and theoretical modeling of the 18o enriched carbon dioxide spectrum by CRDS near 1.74 μm, J. Quant. Spectrosc. Radiat. Transfer 217 (2018) 73–85, http://dx.doi.org/10.1016/j.jqsrt.2018.05.017.

[35] E.V. Karlovets, A. Campargue, D. Mondelain, S. Kassi, S.A. Tashkun, V.I. Perevalov, High sensitivity cavity ring down spectroscopy of^{18}O enriched carbon dioxide between 5850 and 7000 cm^{-1}: Part II — Analysis and theoretical modeling of the $^{12}C^{18}O_2$, $^{13}C^{18}O_2$ and $^{16}O^{13}C^{18}O$ spectra, J. Quant. Spectrosc. Radiat. Transfer 136 (2014) 71–88, http://dx.doi.org/10.1016/j.jqsrt.2013.11.005.

[36] E.V. Karlovets, A. Campargue, S. Kassi, S.A. Tashkun, V.I. Perevalov, Analysis and theoretical modeling of ^{18}O enriched carbon dioxide spectrum by CRDS near 1.35 μm: (II) $^{16}O^{13}C^{18}O$, $^{16}O^{13}C^{17}O$, $^{12}C^{18}O_2$, $^{17}O^{12}C^{18}O$, $^{12}C^{17}O_2$, $^{13}C^{18}O_2$ and $^{17}O^{13}C^{18}O$, J. Quant. Spectrosc. Radiat. Transfer 191 (2017) 75–87, http://dx.doi.org/10.1016/j.jqsrt.2017.01.038.

[37] V. Serdyukov, L. Sinitsa, A. Lugovskoi, Y.G. Borkov, S.A. Tashkun, V.I. Perevalov, LED-based fourier transform spectroscopy of $^{12}C^{16}O^{18}O$ and $^{12}C^{18}O_2$ in the 11 260—11 430 cm^{-1} range, J. Quant. Spectrosc. Radiat. Transfer 177 (2016) 145–151, http://dx.doi.org/10.1016/j.jqsrt.2015.11.024, xVIIIth Symposium on High Resolution Molecular Spectroscopy (HighRus-2015), Tomsk, Russia, https://www.sciencedirect.com/science/article/pii/S0022407315302132.

[38] H. Pan, X.-F. Li, Y. Lu, A.-W. Liu, V.I. Perevalov, S.A. Tashkun, S.-M. Hu, Cavity ring down spectroscopy of^{18}O and^{17}O enriched Carbon Dioxide near 795nm, J. Quant. Spectrosc. Radiat. Transfer 114 (2013) 42–44, http://dx.doi.org/10.1016/j.jqsrt.2012.08.017.

[39] M.J. Reisfeld, H. Flicker, M. Goldblatt, Analysis of the Fourier transform spectra of $^{12}C^{17}O_2$ and $^{12}C^{17}O^{18}O$: The ν_2 (15 μm) region, J. Mol. Spectrosc. 82 (1980) 411–417, http://dx.doi.org/10.1016/0022-2852(80)90124-1.

[40] B.M. Elliott, K. Sung, C.E. Miller, FT-IR spectra of ^{17}O-enriched CO_2 in the ν_3 region: High accuracy frequency calibration and spectroscopic constants for $^{16}O^{12}C^{17}O$, $^{17}O^{12}C^{17}O$, and $^{17}O^{12}C^{18}O$, J. Mol. Spectrosc. 304 (2014) 1–11, http://dx.doi.org/10.1016/j.jms.2014.08.001.

[41] D. Mondelain, E.V. Karlovets, V.I. Perevalov, S.A. Tashkun, A. Campargue, High-sensitivity CRDS absorption spectrum of^{17}O enriched carbon dioxide near 1.74 μm, J. Mol. Spectrosc. 362 (2019) 84–89, http://dx.doi.org/10.1016/j.jms.2019.06.004.

[42] E.V. Karlovets, A. Campargue, D. Mondelain, S. Kassi, S.A. Tashkun, V.I. Perevalov, High sensitivity cavity ring down spectroscopy of^{18}O enriched carbon dioxide between 5850 and 7000 cm^{-1}: Part III Analysis and theoretical modeling of the $^{12}C^{17}O_2$, $^{16}O^{12}C^{17}O$, $^{17}O^{12}C^{18}O$, $^{16}O^{13}C^{17}O$ and $^{17}O^{13}C^{18}O$ spectra, J. Quant. Spectrosc. Radiat. Transfer 136 (2014) 89–107, http://dx.doi.org/10.1016/j.jqsrt.2013.11.006.

[43] D. Jacquemart, Y.G. Borkov, O.M. Lyulin, S.A. Tashkun, V.I. Perevalov, Fourier transform spectroscopy of CO_2 isotopologues at 1.6 μm: Line positions and intensities, J. Quant. Spectrosc. Radiat. Transfer 160 (2015) 1–9, http://dx.doi.org/10.1016/j.jqsrt.2015.03.016.

[44] X. de Ghellinck d'Elseghem Vaernewijck, S. Kassi, M. Herman, $^{17}O^{12}C^{17}O$ and $^{18}O^{12}C^{17}O$ overtone spectroscopy in the 1.64 μm region, Chem. Phys. Lett. 514 (2011) 29–31, http://dx.doi.org/10.1016/j.cplett.2011.08.025.

[45] D. Golebiowski, M. Herman, O. Lyulin, $^{16}O^{12}C^{17}O$ and $^{18}O^{12}C^{17}O$ spectroscopy in the 1.2–1.25 μm region, Can. J. Phys. 91 (2013) 963–965, http://dx.doi.org/10.1139/cjp-2012-0482.

[46] R.A. Toth, C.E. Miller, L.R. Brown, V.M. Devi, D.C. Benner, Line strengths of $^{16}O^{13}C^{16}O$, $^{16}O^{13}C^{18}O$, $^{16}O^{13}C^{17}O$ and $^{18}O^{13}C^{18}O$ between 2200 and 6800 cm^{-1}, J. Mol. Spectrosc. 251 (2008) 64–89, http://dx.doi.org/10.1016/j.jms.2008.01.009.

[47] B.V. Perevalov, V.I. Perevalov, A. Campargue, A (nearly) complete experimental linelist for $^{13}C^{16}O_2$, $^{16}O^{13}C^{18}O$, $^{16}O^{13}C^{17}O$, $^{13}C^{18}O_2$ and $^{17}O^{13}C^{18}O$ by high-sensitivity CW-CRDS spectroscopy between 5851 and 7045 cm^{-1}, J. Quant. Spectrosc. Radiat. Transfer 109 (2008) 2437–2462, http://dx.doi.org/10.1016/j.jqsrt.2008.03.010.

[48] A. Campargue, K.F. Song, N. Mouton, V.I. Perevalov, S. Kassi, High sensitivity CW-Cavity Ring Down Spectroscopy of five$^{13}CO_2$ isotopologues of carbon dioxide in the 1.26-1.44 μm region (I): Line positions, J. Quant. Spectrosc. Radiat. Transfer 111 (2010) 659–674, http://dx.doi.org/10.1016/j.jqsrt.2009.11.013.

[49] S.A. Tashkun, V.I. Perevalov, R.R. Gamache, J. Lamouroux, CDSD-296, high-resolution carbon dioxide spectroscopic databank: An update, J. Quant. Spectrosc. Radiat. Transfer 228 (2019) 124–131, http://dx.doi.org/10.1016/j.jqsrt.2019.03.001.

[50] X. Huang, D.W. Schwenke, R.S. Freedman, T.J. Lee, Ames-2021 CO_2 dipole moment surface and IR line lists: toward 0.1% uncertainty for CO_2 IR intensities, J. Phys. Chem. A 126 (35) (2022) 5940–5964, http://dx.doi.org/10.1021/acs.jpca.2c01291.

[51] E.J. Zak, J. Tennyson, O.L. Polyansky, L. Lodi, N.F. Zobov, S.A. Tashkun, V.I. Perevalov, Room temperature line lists for CO_2 symmetric isotopologues with *ab initio* computed intensities, J. Quant. Spectrosc. Radiat. Transfer 189 (2017) 267–280, http://dx.doi.org/10.1016/j.jqsrt.2016.11.022.

[52] E.J. Zak, J. Tennyson, O.L. Polyansky, L. Lodi, N.F. Zobov, S.A. Tashkun, V.I. Perevalov, Room temperature line lists for CO_2 asymmetric isotopologues with *ab initio* computed intensities, J. Quant. Spectrosc. Radiat. Transfer 203 (2017) 265–281, http://dx.doi.org/10.1016/j.jqsrt.2017.01.037.